Optogenetic stimulation of infralimbic PFC reproduces ketamine's rapid and sustained antidepressant actions

Manabu Fuchikami, Alexandra Thomas, Rongjian Liu, Eric S. Wohleb, Benjamin B. Land, Ralph J. DiLeone, George K. Aghajanian, and Ronald S. Duman[1]

Laboratory of Molecular Psychiatry, Department of Psychiatry, Yale University School of Medicine, New Haven, CT 06508

Ketamine produces rapid and sustained antidepressant actions in depressed patients, but the precise cellular mechanisms underlying these effects have not been identified. Here we determined if modulation of neuronal activity in the infralimbic prefrontal cortex (IL-PFC) underlies the antidepressant and anxiolytic actions of ketamine. We found that neuronal inactivation of the IL-PFC completely blocked the antidepressant and anxiolytic effects of systemic ketamine in rodent models and that ketamine microinfusion into IL-PFC reproduced these behavioral actions of systemic ketamine. We also found that optogenetic stimulation of the IL-PFC produced rapid and long-lasting antidepressant and anxiolytic effects and that these effects are associated with increased number and function of spine synapses of layer V pyramidal neurons. The results demonstrate that ketamine infusions or optogenetic stimulation of IL-PFC are sufficient to produce long-lasting antidepressant behavioral and synaptic responses similar to the effects of systemic ketamine administration.

prefrontal cortex | synapse | neural depolarization | antidepressant | glutamate

The NMDA receptor antagonist ketamine produces rapid and robust therapeutic responses in treatment-resistant (1, 2) as well as bipolar depressed patients (3). Preclinical studies report that ketamine also rapidly increases the number and function of spine synapses in the medial prefrontal cortex (mPFC) and that these effects are associated with rapid antidepressant behavioral responses in rodent models (4). These findings represent a major advance for the treatment of depression, although the widespread use of ketamine is limited by side effects (e.g., psychotomimetic and dissociative symptoms) and abuse potential. Further studies of the mechanisms underlying the actions of ketamine could lead to novel rapid antidepressant treatments with fewer side effects.

Neuroimaging studies in humans demonstrate that ketamine increases the activity of PFC (5–7), consistent with evidence of rapid increases of glutamate transmission in rodent PFC (8, 9). In addition, depressed patients are reported to have reduced activity in the PFC (10) that is normalized with treatment (11). Rodent studies also demonstrate that long-term stress causes neuronal atrophy of mPFC neurons (12, 13) that is rapidly reversed by ketamine (14). Subregions of the mPFC, including infralimbic (IL) and prelimbic (PrL), have been implicated in diverse cognitive and emotional processes, including fear learning, extinction, and anxiety (15–18). However, the role of PFC activity in the behavioral responses to ketamine has not been examined.

Here we examined the antidepressant behavioral effects of neuronal inactivation or direct infusions of ketamine into the IL-PFC and compared these effects with PrL-PFC. Using optogenetics, we also examined the antidepressant and anxiolytic effects of neuronal activation in IL-PFC and determined the impact on pyramidal cell spine number and function to assess long-term neuroplasticity.

Methods and Materials

Animals, Surgery Microinfusions, and Optical Stimulation. Adult male Sprague–Dawley rats (Charles River Laboratories) weighing 150–250 g were pair-housed on a 12-h light/dark cycle (lights on 07:00 h) with food and water available ad libitum. All procedures were done in accordance with the NIH guidelines for the care and use of laboratory animals and the Yale University Institutional Animal Care and Use Committee. Rats were anesthetized with pentobarbital (50 mg/kg, i.p.) and implanted with bilateral guide cannula positioned 1 mm above the site of infusion in either IL [+2.8 mm AP (anteroposterior); ±3.1 mm ML (mediolateral); 3.8 mm DV (dorsoventral); angled at 30°] or PrL (+3.0 mm AP; ±0.50 mm ML; 2.8 mm DV) (12). An angled placement was used for IL. Microinfusions were performed bilaterally into IL or PrL (0.2 µL, 0.1 µL/min) 7 d after surgery. The infusion sites and volumes were based on previous reports demonstrating restricted spread and subregion-specific inactivation following muscimol infusion in the IL or PrL (19, 20). Muscimol (1.25 µg/0.2 µL per hemisphere) or vehicle were microinfused 30 min before ketamine (10 mg/kg, i.p.), a dose that produces antidepressant responses (4). Microinfusion of ketamine included 3, 10, or 30 ng/0.2 µL per hemisphere.

For optogenetic stimulation, rAAV2/CaMKIIa-ChR2(H134R)-eYFP (University of North Carolina Viral Core) or a control vector expressing GFP (rAAV2-GFP, in-house) were infused. Rats were anesthetized with ketamine (80 mg/kg) and xylazine (6 mg/kg); this anesthetic dose of ketamine does not produce antidepressant actions (4). Virus was infused (0.5 µL, 0.1 µL/min) into the IL (+3.2 mm AP; ±0.8 mm ML; 5.5 mm DV) or PrL (+3.2 mm AP; ±0.8 mm ML; 3.0 mm DV) (12), and optical fibers were placed 0.2 mm above the virus injection site and attached to the skull. For optical stimulation, rats were lightly anesthetized (isoflurane) to attach the fiberoptic, and animals with both control and active virus received blue light pulses (pulse width, 15 ms; frequency, 10 Hz; intensity, 5 mW; 473-nm laser) for 60 min (1 min on and 1 min off for 30 cycles). Stimulation settings were based on firing patterns of mPFC pyramidal neurons induced by NMDA receptor antagonism (9) and optogenetic settings necessary to reproduce this firing pattern (21).

Brain Slice Preparation, Recordings, and Spine Analysis. Whole-cell recordings were obtained from layer V pyramidal cells in acute brain slices from rats that had been stereotaxically injected into the IL with rAAV2-ChR2-eYFP or rAAV2-GFP as previously described (14, 22). One day later, brains from stimulated rats were sectioned (400-µm-thick coronal mPFC sections). YFP+ or GFP+ pyramidal neurons in layer V were visualized by infrared differential

interference contrast video microscopy using an Olympus microscope with a 60× lens and YFP filter cube. Neurobiotin (0.3%; Vector Laboratories) was added to the pipette solution to mark selected cells for later processing and imaging. Whole-cell recordings were done with an Axoclamp-2B amplifier (Molecular Devices). Postsynaptic currents were recorded in the continuous single-electrode voltage-clamp mode (3,000 Hz low-pass filter) (*SI Materials and Methods*). Photostimulation of the slice was performed using a 100-mW, 473-nm laser (OEM optics) driven at 10 Hz by an interval generator (pulse width, 15 ms). After completion of recording, slices were processed to visualize spines for analysis. For further details, see *SI Materials and Methods*. Results were expressed as spine density per 10 μm.

Behavioral Studies. Rats were subjected to a series of depression- and anxiety-like behaviors. The forced swim test (FST) was conducted as previously described (4). Briefly, 24 h after preswim, rats received drug treatments or optogenetic stimulation and 24 h later underwent a 10-min test swim; some cases as indicated were subjected to a second test on day 17. Sessions were video recorded and data analyzed by an experimenter blinded to the treatment groups. Total immobility time during the 10-min testing period was analyzed. The novelty-suppressed feeding test (NSFT) is a measure of anxiety that is responsive to chronic administration of typical antidepressants (23) or a single dose of ketamine (4). NSFT was performed as previously described (4) with some modifications. On the test day, rats were placed in an open field (76.5 cm × 76.5 cm × 40 cm; Plexiglas) with a small amount of food in the center. Animals were allowed to explore the open field for 15 min. The latency to approach and consume (seconds) was determined after video recording. Home cage intake was measured as a control. The sucrose preference test (SPT), elevated plus maze, and ambulation tests were conducted as previously described (14).

Histology and Immunohistochemistry. Sections of perfused brains were examined for cannula placements, and animals with incorrect placement were not included. As a measure of neuronal activation, Fos immunoreactivity was determined after microinfusions or optogenetic stimulation (*SI Materials and Methods*).

Statistics. For muscimol microinfusions, two-way analysis of variance (ANOVA) was carried out (factors, microinfusion and systemic injection). For experiments containing three groups, one-way ANOVA was performed, followed by Fisher's protected least significant difference (pLSD) post hoc test ($P < 0.05$). Experiments containing two groups were analyzed by independent t test.

Results

Neuronal Inactivation of IL-PFC Blocks the Effects of Systemic Ketamine. For neuronal silencing, a GABA receptor agonist, muscimol, was infused into IL before systemic injection of ketamine. IL microinfusions were angled to avoid damaging the overlying PrL (Fig. 1). The dose and route of muscimol are based on previous studies of IL as well as PrL in fear extinction (19, 20). Studies to verify neuronal silencing demonstrated that muscimol preinfusion significantly decreases ketamine (i.p.) induction of Fos+ immunolabeling in the IL (Fig. S1). Induction of Fos in the adjacent PrL is also blocked by infusion of muscimol into the IL-PFC, possibly due to silencing of neurons with axon collaterals from IL to PrL.

To determine the influence of neuronal silencing on behavioral responses, muscimol was infused into IL 1 h before systemic ketamine administration, and behavior was assessed 24 h after dosing to avoid the acute effects of drug treatments (Fig. 1 *A–C*). The results demonstrate that muscimol infusion into the IL completely blocks the antidepressant effect of ketamine in the FST (Fig. 1*D*) (interaction, $F_{1,33} = 7.50$, $P < 0.05$). Muscimol infusions into the IL of saline-injected rats had no significant effect on behavior at the time of testing (24 h after infusions) (Fig. 1*B*) ($P = 0.994$). There were no significant effects of muscimol microinfusions into IL on locomotor activity in saline or ketamine-treated rats (determined at the same time as behavioral tests, 24 h after drug treatment) (ANOVA, $F_{2,15} = 0.578$, $P = 0.575$) (Fig. S2). In addition, infusion of muscimol into PrL before ketamine had no effect on the response to systemic ketamine in the FST even though it blocked the
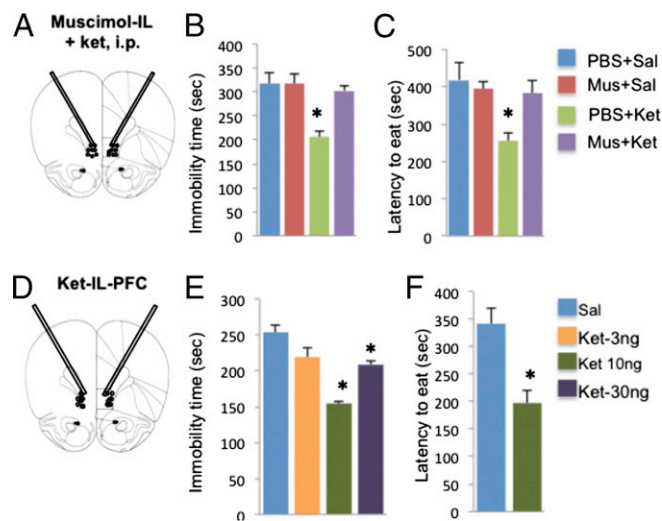

Fig. 1. IL-PFC stimulation is necessary and sufficient for the antidepressant behavioral actions of ketamine. (*A–C*) Neuronal silencing by muscimol infusion (1.25 μg per side) into the IL blocks the effects of ketamine (10 mg/kg, i.p.) in the FST (*B*) and NSFT (*C*). Immobility times in the FST or the latency to eat in NSFT are shown as the mean ± SEM (n = 4–10 per group). *$P < 0.05$, compared with PBS + Sal; analysis of variance (two-way or one-way ANOVA with LSD post hoc test). (*D–F*) Ketamine microinfusions into the IL produce an antidepressant response in the FST (*E*) and an anxiolytic effect in the NSFT (*F*). Doses of 10 and 30 ng per side produced a significant response in the FST, and the 10-ng dose was used for subsequent studies in the NSFT. Means are derived from 4–8 rats per group. *$P < 0.05$, compared with PBS; analysis of variance (one-way ANOVA with LSD post hoc test) or independent t test (*C*, *E*, and *F*). Ket, ketamine; Mus, muscimol; Sal, saline.

induction of Fos in PrL; there was no effect on Fos induction in IL (Figs. S3*B* and S4).

The effect of muscimol infusions on NSFT, a measure of anxiety, was also examined. The latency to feed in a novel environment is decreased by a single dose of ketamine (4) but requires chronic administration of a typical antidepressant (23). Preinfusion of muscimol into the IL completely blocked the effects of ketamine on the latency to feed in the NSFT (interaction, $F_{1,27} = 3.93$, $P < 0.05$; Fig. 1*C*) but had no effect in saline-treated animals.

To further examine the role of IL in the actions of ketamine, the effects of different microinfusion doses (3, 10, and 30 ng, bilateral) were examined. These doses were based on the concentration of ketamine in the brain after systemic injection (24) and the dose required to produce antidepressant responses (4). Ketamine microinfusions into IL produced significant dose-dependent antidepressant effects in the FST (Fig. 1*E*) (ANOVA, $F_{3,16} = 25.690$, $P < 0.01$; LSD post hoc analysis $P < 0.01$ for 10 ng and $P < 0.05$ for 30 ng compared with PBS). The dose–response appears to be an inverted U-shaped curve, similar to the antidepressant behavioral actions of systemic ketamine (4). In the NSFT, microinfusion of ketamine (10 ng) into the IL significantly reduced the latency to feed ($t_{15} = 3.94$, $P < 0.01$; Fig. 1*F*). In contrast, microinfusion of ketamine (10 ng) into PrL had no effect on behavior in either the FST ($P = 0.381$) or latency to feed in the NSFT ($P = 0.410$) (Fig. S3 *D and E*).

In Vitro Characterization of IL Neuronal Optical Stimulation. The requirement for neuronal activation is consistent with reports that ketamine increases extracellular glutamate in the mPFC (8). To directly test if neuronal depolarization of IL produces antidepressant effects, we used an optogenetic approach. For ChR2-induced depolarization of neurons, we infused rAAV2/CaMKIIα-ChR2 (H134R)-eYFP, which responds to blue laser stimulation or control vector (rAAV2-GFP). In vitro brain slice electrophysiology studies were conducted to verify the function of ChR2-eYFP. At the

completion of recording, neurobiotin-labeled cells were stained with streptavidin Alexa594 (red fluorescence); the merged ChR2-eYFP + Alexa594 images appear as yellow (Fig. 2*A*). Patch-clamp recording shows that blue laser stimulation (15 ms pulse width, 10 Hz) consistently produced action potentials triggered by ChR2-induced depolarization (Fig. 2*C*) similar to those induced physiologically in the same cell by a depolarizing pulse (Fig. 2*B*). Voltage-clamp recording in the same cell (Fig. 2*D*) shows the magnitude of ChR2 currents.

The placement of the viral injection cannula in deep layer V is shown in Fig. 2*E* (arrow) (also see Fig. 3*A* and Fig. S5 for viral spread). A zone of ChR2-eYFP signal (green) can also be seen in layer I surrounding the apical tuft dendrites of the recorded cells (Fig. 2*F*), indicating export of ChR2-eYFP to the distal dendrites, which is enhanced as a result of the export signal included in the viral ChR2-eYFP construct. A high-magnification merged confocal image (Fig. 2*G*) illustrates representative images of green punctate fluorescence in close proximity to an apical dendritic branch of one of the recorded cells. Whole-cell recordings show that blue light
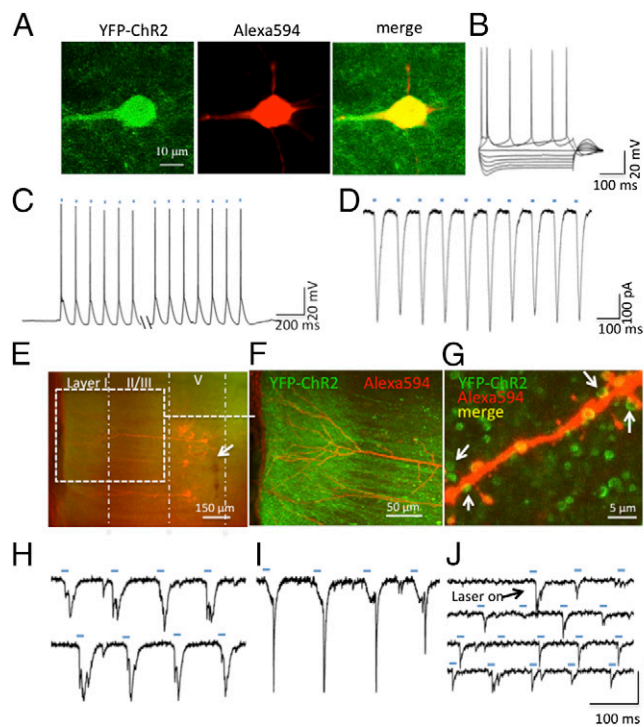

Fig. 2. Electrophysiological validation of ChR2 activity in IL layer V pyramidal cells. (*A*) Two-photon image of a recorded ChR2-eYFP–expressing cell in layer V of IL (green fluorescence, *Left*), colabeling with neurobiotin/strepavidin-Alexa594 (red fluorescence, *Middle*), and merged image showing double labeling (*Right*). (*B*) Spikes induced in this cell by depolarizing pulses. (*C*) Whole-cell recordings showing spikes or (*D*) ChR2 slow-wave currents induced in this cell by laser pulses (15 ms, 10 Hz, marked by blue dashes). (*E*) A low-magnification (5×) fluorescence image in a PFC slice expressing ChR2-eYFP in the IL; a cloud of green fluorescence can be seen both in in the layer I (apical tuft) and in the layer V (cell body) region. Recorded cells are indicated by the presence of Alexa594-labeled cells; arrow shows track of injection needle. (*F*) Confocal image (20×) of the apical shaft and apical tuft of double-labeled recorded cells (expanded from area within white box in *E*). (*G*) High-magnification (100×) merged image shows punctate green ChR2-eYFP fluorescence surrounding an apical branch of a double-labeled recorded cell; arrows show green punctate labeling in close proximity to neurobiotin/Alexa594-labeled spines; these may represent collateral synaptic connections with nearby unlabeled cells. (*H* and *I*) Traces showing laser-induced EPSCs that are evoked in cells with discernable ChR2 slow-wave currents. (*J*) Example of a cell that does not have detectable ChR2 currents but in which laser stimulation evokes EPSCs; note the variable frequency and amplitude of EPSCs by light pulses (blue dashes). The EPSCs may be generated through axon collaterals of neighboring cells that do express ChR2-eYFP.
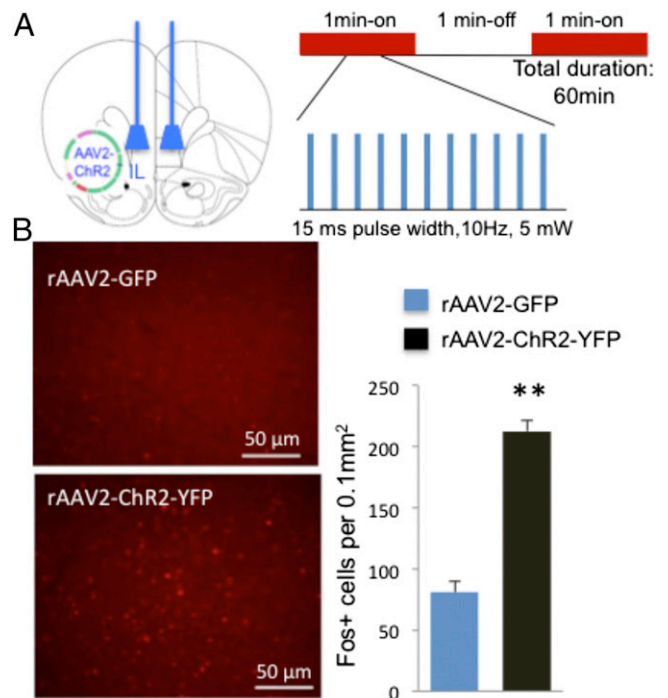

Fig. 3. Optogenetic stimulation of IL and induction of Fos+ labeling. Control (rAAV2-GFP) or active (rAAV2-ChR2-eYFP) viral vectors were infused into the IL-PFC, and 2 wk were allowed for viral infection. (*A*) Location of viral infusions and conditions for in vivo optogenetic stimulation of IL. Both rAAV2-GFP and rAAV2-ChR2-eYFP animals received laser stimulation. (*B*) Influence of laser stimulation on Fos+ cell labeling. Representative images of Fos+ expression after photostimulation of IL in rAAV2-ChR2-eYFP and rAAV2-GFP control animals (×20). (Scale bar, 50 μm.) Optical stimulation in IL significantly increased the number of Fos+ cells in IL (t_{16} = 9.760, P < 0.01).

stimulation (15 ms, 10 Hz lasting 20 s) can evoke EPSCs that overlap with but are distinct from the ChR2-eYFP slow wave currents that are induced in response to the blue light pulses (Fig. 2 *H* and *I*). Interestingly, EPSCs of variable amplitude were also observed in cells that lack detectable ChR2 currents (Fig. 2*J*). These experiments indicate that laser stimulation can affect cells not only directly through activation of ChR2 but also via axon collaterals within the zone of ChR2-eYFP expression.

Optogenetic Stimulation of IL-PFC Produces Antidepressant Behavioral Effects. The effects of in vivo optogenetic stimulation on Fos and antidepressant behavior were examined using laser settings chosen to mimic the effects of systemic ketamine on mPFC pyramidal neuron firing (Fig. 3*A*) (9, 21). Control (rAAV2-GFP) or active (rAAV2-ChR2-eYFP) viruses were infused into the IL as described above, and after recovery a blue light (pulse width, 15 ms; frequency, 10 Hz; intensity, 5 mW) was directed at IL (both control and active virus infused; see Fig. S5*B* for optic fiber location and viral spread). Initial studies examined Fos immunolabeling as a marker of neuronal activity and demonstrate that optogenetic stimulation increases the number of Fos+ cells in IL by ~threefold compared with rats infused with control virus, indicating significant induction of neuronal activation (Fig. 3*B* and Fig. S5*C*). Optogenetic stimulation of IL produced a similar induction of Fos+ cells in PrL, presumably because of axonal projections from IL to this region (Fig. S5*C*).

Using the same conditions, the behavioral effects of IL optical stimulation (active vs. control virus, both receiving blue light pulse; unilateral or bilateral as indicated) were determined (see Fig. 4*A* for sequence of tests). The results demonstrate that optogenetic stimulation of IL-PFC, either unilateral (Uni) or
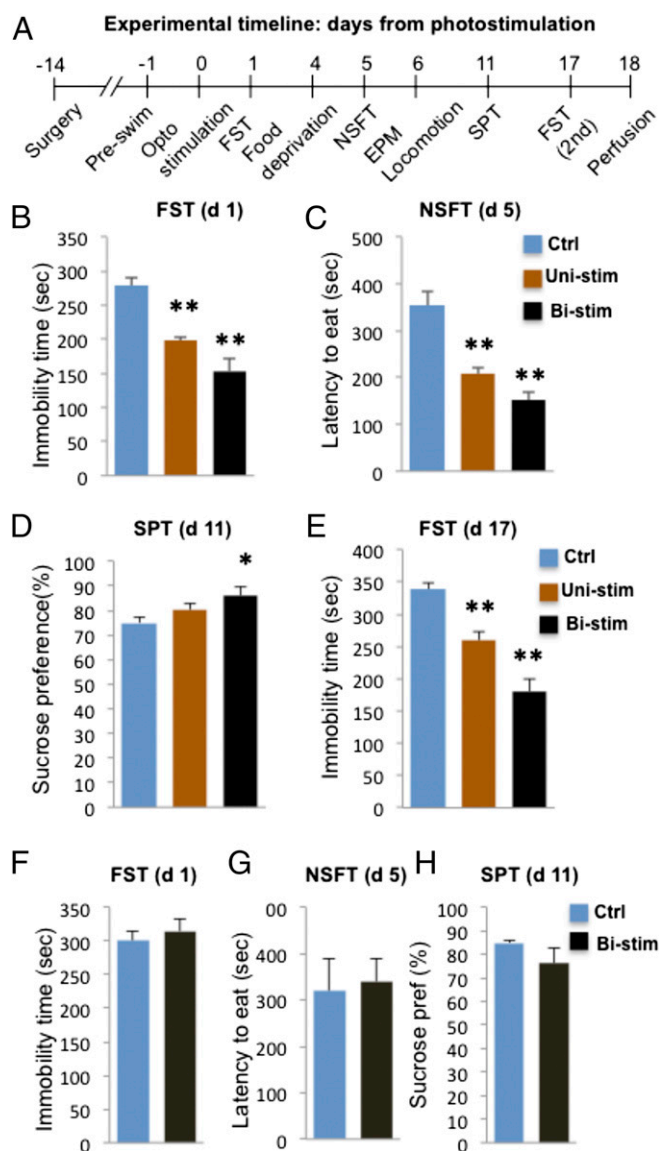
Fig. 4. Photostimulation of IL-PFC produces antidepressant and anxiolytic behavioral responses. (*A*) Timeline for behavioral testing, starting 1 d after laser stimulation. Both rAAV2-GFP and rAAV2-ChR2-eYFP animals received laser stimulation, with the rAAV-GFP serving as controls. Experiments included animals receiving either unilateral (Uni-stim) or bilateral (Bistim) optical stimulation. The results demonstrate that both uni- and bistim of rats infused with rAAV2-ChR2-eYFP produced an antidepressant effect in the FST (*B*) ($F_{2,20}$ = 21.229, P < 0.01) and an anxiolytic effect in the NSFT (*C*) ($F_{2,17}$ = 14.619, P < 0.01) compared with animals receiving rAAV2-GFP control virus and blue light stimulation. Optical stimulation of IL also produced a significant effect in the SPT (*D*), although only in animals receiving bilateral stimulation ($F_{2,21}$ = 3.935, P = 0.037). The antidepressant effect of IL optical stimulation in the FST was still present 17 d after the stimulation (*E*); at this time point, the effect was more robust in the animals receiving bilateral stimulation ($F_{2,20}$ = 35.313, P < 0.01). (*F–H*) In contrast to IL, bilateral stimulation of PrL had no significant effect in the FST (*F*) (t_6 = 0.594, P = 0.574), NSFT (*G*) (t_6 = 0.226, P = 0.829), or SPT (*H*) (t_6 = 1.302, P = 0.241). Data are the mean ± SEM (n = 4–11 per group). *P < 0.05, **P < 0.01 compared with control animals; analysis of variance (one-way ANOVA with LSD post hoc test) or independent t test.

bilateral (Bi), produces rapid, robust, and long-lasting antidepressant effects in the FST (Fig. 4*B*) and anxiolytic effects in the NSFT (Fig. 4*C*). We also found that optical stimulation of IL-PFC (bilateral but not unilateral) resulted in a small but significant increase in the SPT (Fig. 4*D*), a measure of anhedonia

and a core symptom of depression (25). Typically antidepressants reverse the deficits in SPT caused by chronic stress, and the response to optogenetic stimulation could reflect a reversal of surgical stress-induced deficits. In contrast, optogenetic stimulation of PrL had no significant effects on any of these behaviors (Fig. 4 *F–H*). As can be seen in Fig. S6, the viral infusion and optic fiber were targeted to the dorsal aspect of PrL to avoid activation of the underlying IL-PFC, and further studies will be required to determine if more complete activation of the PrL influences antidepressant responses. Optical stimulation of IL or PrL also had no effect on locomotor activity (Fig. S7).

NSFT and SPT were conducted 5 and 11 d after optogenetic stimulation, respectively, demonstrating relatively long-lasting antidepressant behavioral responses. This was confirmed with sustained antidepressant effects in the FST conducted 17 d after either unilateral or bilateral stimulation (Fig. 4*E*). These results demonstrate that a single course of optogenetic stimulation of neurons in IL-PFC induces rapid antidepressant and anxiolytic effects that are long lasting.

Optogenetic Stimulation of IL-PFC in Vivo Increases in Spine Number and Function. Systemic ketamine produces a rapid increase in the number and function of spine synapses in mPFC layer V pyramidal neurons (4). Here we show that optogenetic stimulation of IL also increases spine density 24 h after photo activation (Fig. 5 *A* and *B*); densities are 5.1 ± 0.27 and 6.1 ± 0.19 per 10 μm for control (rAAV2-GFP) and active virus (rAAV2-ChR2-eYFP), respectively (P < 0.05) (Fig. 5*B*). There were no differences in the diameter or length of dendrite segments from control and stimulated neurons (Fig. S8).

Synaptic function of layer V pyramidal cells was assessed by analysis of 5-HT–induced EPSC responses that are highly correlated with spine density and diameter in the apical tuft (22). We found that both the frequency and amplitude of 5-HT–induced EPSCs in layer V pyramidal cells were significantly increased in response to optogenetic stimulation of IL-PFC (rAAV2-ChR2-eYFP) compared with control (rAAV-GFP) (P < 0.05; Fig. 5 *C* and *D*). Significant increases in frequency and amplitude are also shown in cumulative probability distribution curves (Fig. 5*E*). In rAAV2-ChR2-eYFP–infused animals, increases in EPSCs did not differ between ChR2-eYFP+ and ChR2-eYPF-negative cells, suggesting that synaptic up-regulation occurs both through direct excitation of cells expressing ChR2-eYFP and through collateral excitation of ChR2-eYFP-negative cells mediated by local network activation.

Discussion

The results demonstrate that neuronal silencing of IL-PFC blocks the actions of ketamine and that IL-PFC infusion is sufficient for the antidepressant-like effects of ketamine. These findings, combined with up-regulation of the activity marker Fos, indicate that neuronal activity is required for the behavioral actions of ketamine, consistent with evidence of increased extracellular glutamate in the PFC (8). Conversely, the neuronal silencing agent muscimol inhibits the behavioral actions of ketamine, indicating that NMDA receptor blockade at rest is insufficient to produce antidepressant responses, although there are other views (26, 27). A role for neuronal activity is further supported by our results demonstrating that in vivo optogenetic stimulation of IL results in rapid and sustained antidepressant behavioral responses that are associated with increased number and function of spine synapses of layer V pyramidal neurons, similar to the actions of ketamine (4, 14, 28).

Brain slice experiments confirmed that laser stimulation was sufficient to induce spiking in IL-PFC layer V pyramidal neurons that express ChR2-eYFP, as well as adjacent cells, presumably via axon collaterals. This is supported by studies demonstrating that optogenetic stimulation of IL-PFC increases Fos+ cell staining in PrL as well as IL. Similarly, the increase in EPSCs induced by 5-HT in brain slices taken 1 d after in vivo laser stimulation was
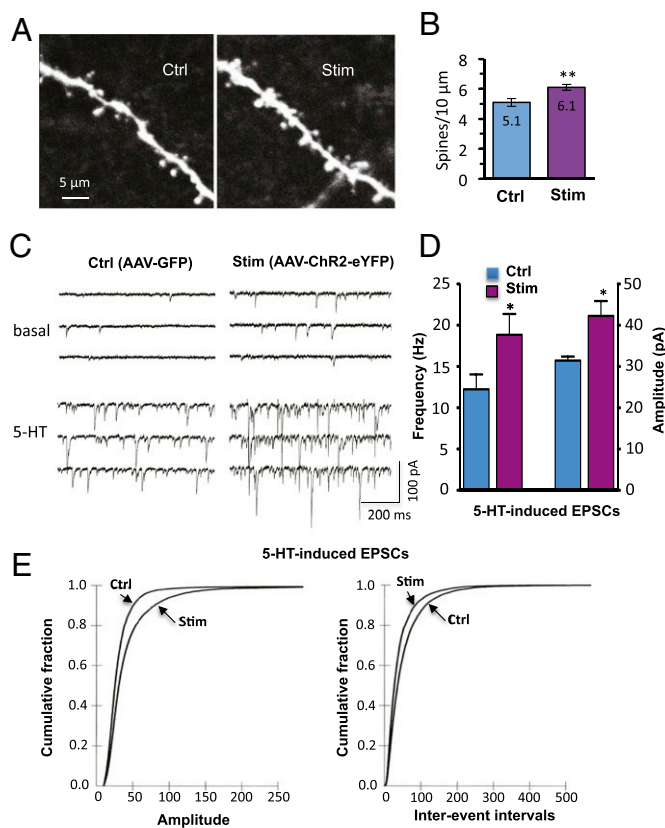
NEUROSCIENCE

Fig. 5. Optogenetic stimulation in vivo increases the number and function of spine synapses in IL-PFC pyramidal neurons. (*A*) Two-photon confocal z-stack projections of apical tuft dendritic segments of layer V pyramidal cells taken from rAAV2-GFP control virus or rAAV2-ChR2-eYFP–infused animals, both receiving in vivo light stimulation. (Scale bar, 10 μm.) (*B*) Spine density analysis; the results are the mean ± SEM (45 images from 11 cells from 5 rats for control; 66 images from 15 cells from 5 rats for stimulated; **$P < 0.01$; Student *t* test). (*C*) Examples of layer V pyramidal cell recording traces taken from control or stimulated animals; note the marked 5-HT–induced EPSCs in the cell taken from the stimulated animal. (*D*) Summary data showing both increased frequency (12.2 ± 1.8 and 18.8 ± 2.5 Hz, control and stimulated, respectively; $P < 0.05$) and amplitude (31.4 ± 1 and 42.3 ± 3.5 pA, respectively; $P < 0.05$) of 5-HT–induced EPSCs (*$P < 0.05$; Student *t* test; $n = 15$ neurons). (*E*) Cumulative probability distributions showing significant increases in amplitude (Kolmogorov–Smirnov two-sample test; $P < 0.0000$; z value = 12.9) and frequency (Kolmogorov–Smirnov two-sample test; $P < 0.0000$; z value = 10.9) of 5-HT–induced EPSCs ($n = 15$ neurons per group).

independent of whether or not a particular recorded cell expressed ChR2. These results are consistent with the idea that pyramidal neurons are embedded in complex, recurrent microcircuits (29–31) and that optogenetic activation of a core group of cells produces broader changes in network function that could underlie the observed behavioral responses.

Optogenetic stimulation of the PFC or target regions receiving ChR2 terminals from PFC neurons is reported to produce antidepressant behavioral responses but only during the stimulation period (32–35). The current study was designed to determine if stimulation of glutamatergic neurons in mPFC could lead to rapid

and sustained synaptogenic and behavioral responses similar to the effects of systemic ketamine. The results are consistent with this hypothesis, demonstrating that IL-PFC photostimulation results in rapid and sustained antidepressant and anxiolytic behavioral responses and increased number and function of spine synapses of layer V pyramidal neurons.

There are several target regions and circuits that could contribute to the actions of ketamine infusion or optogenetic stimulation of IL-PFC. Connections between IL-PFC and amygdala have been implicated in fear memory, extinction, and anxiety and could thereby contribute to the behavioral responses observed in the present study (36, 37). In addition, previous studies demonstrate that mPFC connections with the dorsal raphe or mesolimbic dopamine system, including the nucleus accumbens, could contribute to the antidepressant responses to ketamine and optogenetic stimulation (32, 35, 38, 39). One report has demonstrated that optogenetic stimulation of mPFC terminal fields can produce either antidepressant (dorsal raphe) or prodepressive (lateral habenula) responses, although behavior was examined during photostimulation and did not distinguish between IL and PrL subregions (35). Nevertheless, these results demonstrate the functional complexity of mPFC circuitry in depression and antidepressant responses. Future studies will be needed to examine the interaction of IL-PFC projection neurons with these potential target brain regions to characterize the neuronal circuitry underlying the persistent antidepressant actions of ketamine and optical stimulation. It is also possible that other behavioral actions of ketamine—notably the beneficial neurocognitive effects (40, 41)—are mediated by other cortical regions, such as the anterior cingulate, that warrant investigation.

The results also raise several issues. First, we found that muscimol alone had no effect on behavior, in contrast to a previous report showing that IL-PFC muscimol reduced immobility (42). This difference is likely due to the time point for behavioral analysis: 24 h in the current study versus immediately after muscimol in the previous report. Second, we used unstressed animals, and further studies using chronic stress or social defeat models are needed. Third, we find that optogenetic stimulation of IL-PFC neurons is effective, whereas a previous study shows that electrical stimulation of IL-PFC produces antidepressant actions even when neurons are chemically ablated, suggesting a role for activation of fibers of passage (43). Fourth, an anesthetic dose of ketamine has no effect on antidepressant behaviors and was used for surgeries (4), so studies will be needed to test if prior exposure to high doses of ketamine impact subsequent optogenetic responses.

The results of the current study contribute to a further understanding of the cellular mechanisms underlying the actions of ketamine, but the initial targets and actions by which ketamine produces a burst of glutamate that triggers rapid synaptic and behavioral responses remain unclear. Current approaches using cell-specific techniques to knockdown NMDA receptor subtypes on different populations of glutamate and GABA neurons in the PFC are being conducted to address this question. These experiments combined with studies of circuitry, will elucidate the cellular mechanisms underlying the actions of ketamine and could provide novel targets for safer antidepressant medications.

1. Berman RM, et al. (2000) Antidepressant effects of ketamine in depressed patients. *Biol Psychiatry* 47(4):351–354.
2. Zarate CA, Jr, et al. (2006) A randomized trial of an N-methyl-D-aspartate antagonist in treatment-resistant major depression. *Arch Gen Psychiatry* 63(8):856–864.
3. Diazgranados N, et al. (2010) A randomized add-on trial of an N-methyl-D-aspartate antagonist in treatment-resistant bipolar depression. *Arch Gen Psychiatry* 67(8):793–802.
4. Li N, et al. (2010) mTOR-dependent synapse formation underlies the rapid antidepressant effects of NMDA antagonists. *Science* 329(5994):959–964.
5. Långsjö JW, et al. (2003) Effects of subanesthetic doses of ketamine on regional cerebral blood flow, oxygen consumption, and blood volume in humans. *Anesthesiology* 99(3):614–623.
6. Långsjö JW, et al. (2004) Effects of subanesthetic ketamine on regional cerebral glucose metabolism in humans. *Anesthesiology* 100(5):1065–1071.
7. Holcomb HH, Lahti AC, Medoff DR, Cullen T, Tamminga CA (2005) Effects of non-competitive NMDA receptor blockade on anterior cingulate cerebral blood flow in volunteers with schizophrenia. *Neuropsychopharmacology* 30(12):2275–2282.

8. Moghaddam B, Adams B, Verma A, Daly D (1997) Activation of glutamatergic neurotransmission by ketamine: A novel step in the pathway from NMDA receptor blockade to dopaminergic and cognitive disruptions associated with the prefrontal cortex. *J Neurosci* 17(8):2921–2927.

9. Homayoun H, Moghaddam B (2007) NMDA receptor hypofunction produces opposite effects on prefrontal cortex interneurons and pyramidal neurons. *J Neurosci* 27(43): 11496–11500.

10. Price JL, Drevets WC (2010) Neurocircuitry of mood disorders. *Neuropsychopharmacology* 35(1):192–216.

11. Murrough JW (2012) Ketamine as a novel antidepressant: From synapse to behavior. *Clin Pharmacol Ther* 91(2):303–309.

12. Bessa JM, et al. (2009) The mood-improving actions of antidepressants do not depend on neurogenesis but are associated with neuronal remodeling. *Mol Psychiatry* 14(8): 764–773, 739.

13. Izquierdo A, Wellman CL, Holmes A (2006) Brief uncontrollable stress causes dendritic retraction in infralimbic cortex and resistance to fear extinction in mice. *J Neurosci* 26(21):5733–5738.

14. Li N, et al. (2011) Glutamate N-methyl-D-aspartate receptor antagonists rapidly reverse behavioral and synaptic deficits caused by chronic stress exposure. *Biol Psychiatry* 69(8):754–761.

15. Holmes A, Wellman CL (2009) Stress-induced prefrontal reorganization and executive dysfunction in rodents. *Neurosci Biobehav Rev* 33(6):773–783.

16. Seamans JK, Lapish CC, Durstewitz D (2008) Comparing the prefrontal cortex of rats and primates: Insights from electrophysiology. *Neurotox Res* 14(2-3):249–262.

17. Sotres-Bayon F, Quirk GJ (2010) Prefrontal control of fear: More than just extinction. *Curr Opin Neurobiol* 20(2):231–235.

18. Senn V, et al. (2014) Long-range connectivity defines behavioral specificity of amygdala neurons. *Neuron* 81(2):428–437.

19. Laurent V, Westbrook RF (2009) Inactivation of the infralimbic but not the prelimbic cortex impairs consolidation and retrieval of fear extinction. *Learn Mem* 16(9): 520–529.

20. Sierra-Mercado D, Padilla-Coreano N, Quirk GJ (2011) Dissociable roles of prelimbic and infralimbic cortices, ventral hippocampus, and basolateral amygdala in the expression and extinction of conditioned fear. *Neuropsychopharmacology* 36(2): 529–538.

21. Ji G, Neugebauer V (2012) Modulation of medial prefrontal cortical activity using in vivo recordings and optogenetics. *Mol Brain* 5:36.

22. Liu RJ, Aghajanian GK (2008) Stress blunts serotonin- and hypocretin-evoked EPSCs in prefrontal cortex: Role of corticosterone-mediated apical dendritic atrophy. *Proc Natl Acad Sci USA* 105(1):359–364.

23. Santarelli L, et al. (2003) Requirement of hippocampal neurogenesis for the behavioral effects of antidepressants. *Science* 301(5634):805–809.

24. Mickley GA, et al. (1998) Ketamine blocks a conditioned taste aversion (CTA) in neonatal rats. *Physiol Behav* 64(3):381–390.

25. Willner P (2005) Chronic mild stress (CMS) revisited: Consistency and behavioural-neurobiological concordance in the effects of CMS. *Neuropsychobiology* 52(2): 90–110.

26. Autry AE, et al. (2011) NMDA receptor blockade at rest triggers rapid behavioural antidepressant responses. *Nature* 475(7354):91–95.

27. Kavalali ET, Monteggia LM (2015) How does ketamine elicit a rapid antidepressant response? *Curr Opin Pharmacol* 20:35–39.

28. Liu RJ, et al. (2013) GSK-3 inhibition potentiates the synaptogenic and antidepressant-like effects of subthreshold doses of ketamine. *Neuropsychopharmacology* 38(11): 2268–2277.

29. Turrigiano GG, Nelson SB (2004) Homeostatic plasticity in the developing nervous system. *Nat Rev Neurosci* 5(2):97–107.

30. Campanac E, Debanne D (2007) Plasticity of neuronal excitability: Hebbian rules beyond the synapse. *Arch Ital Biol* 145(3-4):277–287.

31. Haider B, McCormick DA (2009) Rapid neocortical dynamics: Cellular and network mechanisms. *Neuron* 62(2):171–189.

32. Chaudhury D, et al. (2013) Rapid regulation of depression-related behaviours by control of midbrain dopamine neurons. *Nature* 493(7433):532–536.

33. Covington HE, 3rd, et al. (2010) Antidepressant effect of optogenetic stimulation of the medial prefrontal cortex. *J Neurosci* 30(48):16082–16090.

34. Tye KM, Deisseroth K (2012) Optogenetic investigation of neural circuits underlying brain disease in animal models. *Nat Rev Neurosci* 13(4):251–266.

35. Warden MR, et al. (2012) A prefrontal cortex-brainstem neuronal projection that controls response to behavioural challenge. *Nature* 492(7429):428–432.

36. Myers-Schulz B, Koenigs M (2012) Functional anatomy of ventromedial prefrontal cortex: Implications for mood and anxiety disorders. *Mol Psychiatry* 17(2):132–141.

37. McLaughlin RJ, Hill MN, Gorzalka BB (2014) A critical role for prefrontocortical endocannabinoid signaling in the regulation of stress and emotional behavior. *Neurosci Biobehav Rev* 42:116–131.

38. Russo SJ, Nestler EJ (2013) The brain reward circuitry in mood disorders. *Nat Rev Neurosci* 14(9):609–625.

39. Tye KM, et al. (2013) Dopamine neurons modulate neural encoding and expression of depression-related behaviour. *Nature* 493(7433):537–541.

40. Salvadore G, et al. (2010) Anterior cingulate desynchronization and functional connectivity with the amygdala during a working memory task predict rapid antidepressant response to ketamine. *Neuropsychopharmacology* 35(7):1415–1422.

41. Murrough JW, et al. (2013) Neurocognitive effects of ketamine in treatment-resistant major depression: Association with antidepressant response. *Psychopharmacology (Berl)*.

42. Slattery DA, Neumann ID, Cryan JF (2011) Transient inactivation of the infralimbic cortex induces antidepressant-like effects in the rat. *J Psychopharmacol* 25(10): 1295–1303.

43. Hamani C, et al. (2010) Antidepressant-like effects of medial prefrontal cortex deep brain stimulation in rats. *Biol Psychiatry* 67(2):117–124.

NEUROSCIENCE